Segmentation and Reconstruction of Cerebral Vessels from 3D Rotational Angiography for AVM Embolization Planning

Fan Li, Yasmina Chenoune, Meriem Ouenniche, Raphaël Blanc, Eric Petit

Abstract— **Diagnosis and computer-guided therapy of cerebral Arterio-Venous Malformations (AVM) require an accurate understanding of the cerebral vascular network both from structural and biomechanical point of view. We propose to obtain such information by analyzing three Dimensional Rotational Angiography (3DRA) images. In this paper, we describe a two-step process allowing 1) the 3D automatic segmentation of cerebral vessels from 3DRA images using a region-growing based algorithm and 2) the reconstruction of the segmented vessels using the 3D constrained Delaunay Triangulation method. The proposed algorithm was successfully applied to reconstruct cerebral blood vessels from ten datasets of 3DRA images. This software allows the neuroradiologist to separately analyze cerebral vessels for pre-operative interventions planning and therapeutic decision making.**

I. Introduction

A. Background and Purpose

The cerebral vascular network is very complex, as seen through its geometrical structure and its biomechanical organization; particularly in case of lesions or diseases. Consequently, practitioners need high-quality images to perform both diagnosis and computer-guided therapy. In a normal brain, arteries communicate with veins through arterioles and small capillaries. A cerebral Arterio-Venous Malformation (AVM) occurs when the arteries connect directly with the veins without any intervening capillary network. This results in venous engorgement and dilation or stenosis leading to a high risk of intracranial hemorrhage. Advanced imaging and 3D visualization of brain vessels are very important for AVM diagnosis and management. Indeed, the treatment highly depends on the AVM size and location in addition of patient age and general health. Conservative treatment with clinical follow-up or curative treatment will then be chosen [1]. The embolization [2] which consists in the occlusion of the arterial feeders and the AVM nidus thanks to an embolic agent can be performed alone or in conjunction with other modalities. It is carried out by a neuroradiologist using micro-catheters to navigate throughout the intracranial arterial feeders until the nidus. In the last few years, the 3D Rotational Angiography (3DRA) was considered as a promising imaging technique for vessels visualization and became the reference imaging modality in neurovascular interventions. Indeed, this imaging technique provides 3D high-resolution images of the whole vascular tree, allowing a detailed anatomic analysis of the arterial supply of AVMs. However, the visual tracking of a specific vessel with its branches during the pre-operative interventions planning is difficult on such images, due to the complexity and the tangle of the vessels. To deeply track a vessel, the neuroradiologist needs a new vessel representation obtained by isolating a specific vessel from the rest of the vascular tree.

The present work aims to provide an efficient software to facilitate the pre-operative 3D analysis of the AVM feeding arteries and draining vessels. For this purpose, an innovative method for the 3D segmentation and reconstruction of cerebral vessels from 3DRA images is proposed. The novelty of this research compared to previous work lies in the 3D implementation of the region-growing segmentation process, applied to 3DRA images. In addition, our application offers the possibility to intervene on the reconstructed image to isolate a specific vessel, visualize it in different angles and make quantitative measurements. To our knowledge, no previous work has dealt with this issue.

B. Vascular Network Segmentation

Cerebral vessels are complex objects by their shapes, sizes and tree organization/overlapping. Consequently, the vascular network segmentation is not an easy task. Several methods for the extraction of vascular structures have been proposed. The choice of the most suitable one depends on the imaging modality and on the intended application [3, 4]. Among these methods, pattern recognition-based approaches, which can operate in a multi-scale way [5, 6] were proposed. Other methods using the extraction of the vessels centerline were also largely used to reconstruct the vessels skeleton [7, 8], along with the inclusion of methods based on the contours-intensity information [9]. Some authors proposed advanced global or adaptive thresholding-based approaches to segment the vascular tree [10] or cerebral aneurisms. Such approaches were applied either on 3DRA, magnetic resonance angiography (MRA) or computed tomography angiography (CTA) images [11]. Morphological tools have also been used to segment 3D-CTA images of AVM [12], but these approaches require low noise images. Moreover, model-based methods such as Geodesic Active Regions (GAR) or level sets were used for an automated segmentation of cerebral vasculature in 3DRA [13, 14] or for cerebral aneurysms segmentation in 3DRA and CTA [15]. These implicit methods provide good results but are very sensitive to the parameters setting, and are very time consuming, being implemented with an iterative process. Artificial intelligence was recently used for AVMs segmentation from MR angiographic images [16]. The region-growing method was also applied to segment the coronary tree in CT angiographic

Research supported by ESME Sudria Engineering School.

Fan LI, Yasmina CHENOUNE and Meriem OUENNICHE are with the Laboratoire Ingénierie des Systèmes de Traitement de l'Information, ESME Sudria, Ivry-Sur-Seine, France (e-mail: corresponding author li@esme.fr, chenoune@esme.fr).

Raphaël BLANC is with the Fondation Ophtalmologique de Rothschild, Paris, Interventional Neuroradiology, France (e-mail: rblanc@gmail.com).

Eric PETIT is with the Laboratoire Images, Signaux et Systèmes Intelligents, Créteil, France (e-mail : eric.petit@u-pec.fr).

images [17] and to extract the cerebral vessels from 3DRA images [18]. The region-growing algorithm evolution is controlled by a homogeneity criterion and by the research of local similarities in pixels/voxels neighborhood. To deliver reliable results, this algorithm requires highly contrasted vessels otherwise it often fails. Furthermore, it usually has to be manually initialized. Due to the use of a contrast agent, a high uniformity of intensity in the vessels is observed on the 3DRA images, compared to other brain tissues. Consequently, we propose to perform the vessels segmentation with a 3D region-growing algorithm.

C. Vascular Network Reconstruction

To reconstruct the vessels surface for visualization, several methods depending on the segmentation outcome and on mesh generation methods have been proposed. Model-based or model-free surface modeling techniques were implemented [19]. The model-based techniques which assume some model assumptions, in particular a circular cross-section generally require the centerline extraction from segmented vessels [20] and geometric primitives such as cylinders [21] are used to fit the vessels surface. However, the accuracy of the generated surfaces which present a low visual quality might not be sufficient for the diagnosis of pathologic structures. The model-free surface representations require no assumptions and exploit the segmentation results to construct a set of points from which smooth surfaces are obtained. A higher accuracy can thus be achieved with the Marching Cubes or the Constrained Elastic Surface Nets methods [22]. As our region-growing algorithm provided high-quality segmentation results, we propose to simply reconstruct the vessels surface by converting the set of 2D vessels contours resulting from the segmentation step, to a 3D mesh using the constrained Delaunay triangulation method.

II. Material and Methods

A. Patients and 3DRA Acquisitions

Ten patients (age range: 27- 62, mean age: 44 years, 40% women) with brain AVM underwent 3DRA imaging. Acquisitions were performed with a Philips Allura angiographic unit (Philips Healthcare, Best, The Netherlands), after the injection of 28 cm^3 of contrast agent to enhance the vessels, at 4 cm^3/second with a rotation of 210° and a delay of 3 seconds between injection and acquisition. The size of the resulted images was 256x256x256 pixels/image with cubic voxel size varying from 0.29 to 0.49 mm^3. The Philips Allura angiographic unit delivers initial reconstructions in 4 seconds.

B. Automated Seeds Selection

The 3D region-growing algorithm is initialized by automatic seeds localization on the binarized and filtered first slice of the 3DRA volume.

Binarization and Noise Filtering

An example of a 3DRA axial slice is given in Fig.1(a). Pixels intensity distribution can be divided into two classes: vessel and background [23]. In order to obtain markers of the vessels, a thresholding method using the morphological geodesic reconstruction [24] was applied. Let I be a grayscale image and $Thres_{low}$ and $Thres_{high}$ two thresholds $(Thres_{low} < Thres_{high})$. The binarization results of I from the two thresholds are, respectively named J and K. Let $J_1, J_2, \dots J_m$ be the connected components of J and $K_1, K_2, \dots K_m$ be the connected components of K. Since it is easily proved that $K \subseteq J$, K is called marker and J is called mask. The reconstruction $R_{J(k)}$ of mask J from marker K is the union of the connected components of J which contains at least one common pixel with K:

$$R_{J(k)} = \bigcup_{K \cap J_i \neq \emptyset} J_i \quad (1)$$

The lower threshold allows separating the different regions of the image while the upper threshold is used to mark some points in each potential vessel. On the resulting binary image, the small structures are removed by considering a size parameter S, to keep only pixels belonging to the vessels.

Location of Region-Growing Seed Points

The centers of the extracted regions are then defined as the seeds. The center of mass was usually considered as the seed in some previous work [18]. Nevertheless, the forms of vessels are not always convex and the center of mass may be located outside the region. For that reason, we considered a center which should be strictly inside the region. In a binary image I, let R be one region of interest which contains N sets of pixels p_i $(i = 1, 2, \dots, N)$. For each pixel p_i in R, the sum of all the distances $D(p_i)$ from this point to all the other pixels p_j is defined as follows:

$$D_{(p_i)} = \sum_{j=1}^{N} \left(|x_i - x_j| + |y_i - y_j| \right) \quad (2)$$

with (x_i, y_i) and (x_j, y_j) respectively the p_i and p_j coordinates. The central point p_{center} is obtained such as:

$$p_{center} = \underset{i=1,\dots N}{Argmin}\, D_{(p_i)} \quad (3)$$

C. 3D Region-Growing Vessels Segmentation

Once the seeds markers are successfully selected on the first slice, we apply the 3D region-growing method to segment a given branch, by selecting one seed from all the defined markers. The algorithm evolution depends on a region membership criterion. Because of the uniformity of the voxels intensity on the 3DRA images, a voxel intensity criterion is used. Let I_{max} and I_{min} denote separately the greatest and the lowest gray level of voxels in the whole volume. Let the voxel $p_i(x_i, y_i, z_i)$ be the initial seed point, $I(p_i)$ be the intensity value of p_i. Each 6-connected neighbor p_j of p_i is labeled as the same vessel as p_i if the following condition is satisfied:

$$\left| I(p_i) - I(p_j) \right| < T * |I_{max} - I_{min}| \quad (4)$$

with $I(p_j)$ the intensity of p_j and T a weighting parameter.

When the condition (4) is verified for a neighbor p_j of p_i, the process is iterated for the six neighbors of the voxel p_j. This process ends when no changes occur after two successive iterations. Once the 3D region-growing process is completed, the 2D contours of the segmented vascular structures are extracted slice by slice. They will be exploited, to reconstruct the 3D mesh using the 3D Delaunay Triangulation [25].

D. 3D Vessels Reconstruction

An algorithm for creating a 3D mesh that tightly fits the external surface of the vessels is proposed. It is based on the constrained Delaunay triangulation and converts the set of 2D vessels contours resulting from our region-growing algorithm, to a 3D mesh, constituted of non-overlapping triangles that represent the surface of the vessels.

This algorithm establishes a correspondence between selected points from each two successive contours, belonging to the same vessel (see example on Fig.2 (b)). Since the vessels sections are not always convex, the triangulation is constrained by the contours to avoid problems of external triangles construction. The implemented algorithm is able to reconstruct vessels with various forms and sizes and also to identify vessels divisions into two branches (bifurcations).

III. Results and Discussion

Our segmentation and reconstruction algorithm was applied on a region of interest for each 3DRA image of our dataset. First, the seeds are automatically selected from the first image of the considered stack of slices. The user is then asked to choose the vessel he wishes to reconstruct. Then, the region-growing algorithm starts from the corresponding seed point and propagates through the 3D volume in order to carry out the vessel segmentation. Blood vessels with different sizes and shapes as well as multiple bifurcations have been successfully reconstructed. Furthermore, the exploration of the voxel neighborhood in the three spatial directions allows the automated detection of vessels bifurcations, which is very important for the complete visualization of a given vessel with all its branches.

For each processed dataset, the analysis of the logarithmic histogram of the 3D image [13] allows the determination of the suitable $Thres_{low}$ and $Thres_{high}$ values used in the first step for automated seeds selection. The filtering process enables the detection of all the vascular structures and removes most of noise components (see Fig.1.(c)).

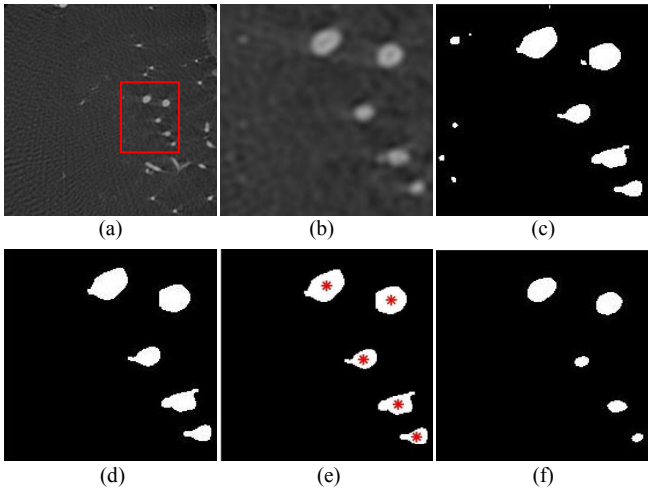

Figure 1. Segmentation results after the binarization and filtering steps for a 3DRA image, (a) A 3DRA slice, (b) zoom-in on a region of interest containing vascular structures, (c) the obtained binary image for the normalized threshold values $Thres_{low}$=0.28 and $Thres_{high}$=0.43, (d) the filtered binary image with S=6, (e) the detected seeds points and (f) the final region-growing segmented vascular structures from the seed points.

The remaining noise is simply filtered by eliminating the structures smaller than a given size *S*. The *S* parameter represents the total number of pixels over the small region and allows computing the area of the smallest vessel section that can be segmented. In the example of Fig.1, the image resolution was of 0.35 mm and the size parameter *S* which controls noise filtering was fixed to 6 pixels. Consequently, vessels with a small diameter of 0.96 mm were successfully segmented. The finest reconstructed vessel diameter that was reached by our algorithm, on all datasets was 0.7 mm.

The segmentation results were slightly sensitive to the value of the *T* weighting parameter, which controls the membership criterion in the region-growing process. This parameter was adjusted for each dataset and was experimentally fixed between 6% and 8%. Three examples of 3D vessels reconstructions, computed for three different patients are illustrated by Fig.2 and Fig.3.

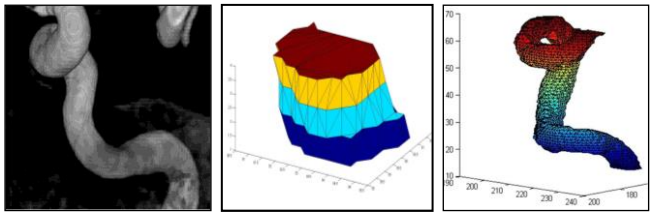

Figure 2. (a) Part of the internal carotid artery reconstructed from 60 3DRA slices with the Philips Allura unit, (b) example of a 3D mesh obtained after the 2D to 3D Delaunay reconstruction of four successive contours, (c) the obtained 3D constrained Delaunay reconstruction result for this vessel.

First, the Internal Carotid Artery (ICA) is reconstructed from a set of 60 3DRA slices (Fig. 2). The obtained result shown by Fig.2.(c) was visually compared to the reconstruction obtained with the angiographic unit Fig.2.(a) by a neuroradiologist. We can easily see that this part of vessel was successfully reconstructed. Another example shows the reconstruction of the two branches of the Anterior Cerebral Artery (ACA) from 120 3DRA slices (Fig. 3). Different viewing angles allow for a greater visualization of the vessels bifurcations. We also show on Fig.3(e-f) vessel reconstruction results obtained with our algorithm in comparison with the corresponding Maximum Intensity (MIP) images. Thus, the whole process including the 3D segmentation followed by the Delaunay reconstruction was able to automatically reconstruct a vessel in 3 or 4 seconds. Moreover, the process depends on few parameters whose values are mostly fixed for all the 3DRA data.

IV. Conclusion

In this paper, a new method dedicated to the detailed visual analysis of cerebral vessels from 3DRA slices is presented. The whole process includes a segmentation based on a 3D region-growing method and followed by a 3D reconstruction using the constrained Delaunay triangulation. The obtained results on ten patients with AVM demonstrate the efficiency of our method that allows the reconstruction of a given vascular structure with its branches and with a high precision. The visualization is highly improved since we obtain a simplified representation in which the initial tangle of vessels is reduced. This new vessel representation might be

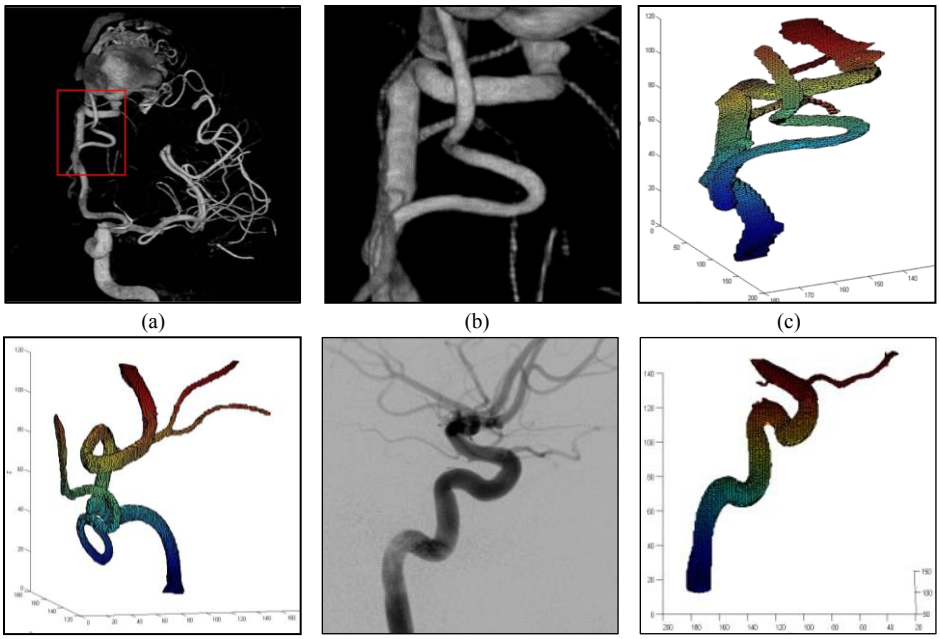

Figure 3. Examples of vessels reconstruction, (a) the reconstructed vessel tree with the Philips Allura unit, (b) zoom-in of the Anterior Cerebral Artery (ACA), (c) ACA reconstruction from 120 3DRA slices using the proposed method with the same view angle, (d) visualization from another angle of view and an example of (f) vessel reconstruction using our algorithm in comparison with (e) the Maximum Intensity (MIP) corresponding image.

of major usefulness for neuroradiologists to guide AVM management and to aid for pre-operative interventions planning. We are currently extending this work on an enlarged database to confirm the efficiency of our algorithm and to assess its relevance in a clinical context. In future, our aim is to enrich the virtual vessel object that we built, by biomechanical measurements such as intracranial blood pressure in order to modelize the vascular network.

REFERENCES

[1] C.S. Ogilvy, *et al.*, "AHA Scientific Statement: Recommendations for the management of intracranial arteriovenous malformations: a statement for healthcare professionals from a special writing group of the Stroke Council, American Stroke Association," *Stroke,* vol. 32, pp.1458-1471, 2001.

[2] D. Lesage, *et al.*, "A review of 3D vessel lumen segmentation techniques: models, features and extraction schemes," *Medical Image Analysis,* vol. 13, pp. 819-45, 2009.

[3] P. Gailloud, "Endovascular treatment of cerebral arteriovenous malformations," *Tech Vasc. Interv Radiol.,* vol. 8, pp. 118-28, 2005.

[4] C. Kirbas and F. Quek, "A review of vessel extraction techniques and algorithms," *ACM Computing Surveys,* vol. 36, pp. 81-121, 2004.

[5] A. F. Frangi, *et al.*, "Multiscale vessel enhancement filtering," in *MICCAI*, pp. 130-137, 1998.

[6] M. Chwialkowski, "A method for fully automated quantitative analysis of arterial flow using flow-sensitized MR images," *Computerized Medical Imaging and Graphics,* vol. 20, pp. 365-378, 1996.

[7] W. Wong and A. Chung, "Probabilistic vessel axis tracing and its application to vessel segmentation with stream surfaces and minimum cost paths," *Medical Image Analysis,* vol. 11 (6), pp. 567-587, 2007.

[8] Y. Kawata, *et al.*, "An approach for detecting blood vessel diseases from cone-beam CT image," in *IEEE Int. Conf. on Image Processing*, vol.2, pp. 500-503.1995.

[9] E. Bullitt, *et al.*, "Symbolic description of intracerebral vessels segmented from MRA and evaluation by comparison with X-ray angiograms," *IEEE Med. Image Anal.,* vol. 5, pp. 157-169, 2001.

[10] M. H. F. Wilkinson, "Gaussian-weighted moving window robust automatic threshold selection," *Lecture Notes in Computer Science,* vol. 2756, pp. 369-376, 2003.

[11] C. M. Hentschke, *et al.*, "Detection of cerebral aneurysms in MRA, CTA and 3D-RAdata sets," in *Proc. SPIE, Medical Imaging 2012: Computer-Aided Diagnosis*, pp. 83151I-83151I-7, 2012.

[12] D. Babin, *et al.*, "Generalized pixel profiling and comparative segmentation with application to arteriovenous malformation segmentation," *Medical Image Analysis,* vol. 16, pp. 991-1002, 2012.

[13] H. Bogunovic, *et al.*, "Automated Landmarking and Geometric Characterization of the Carotid Siphon," *Medical Image Analysis,* vol. 16, pp. 889-903, 2012.

[14] D. Nain, *et al.*, "Vessel segmentation using a shape driven flow," In *Intl. Conf. on Medical Image Computing and Comp. Ass. Intervention (MICCAI)*, pp. 51-59, 2004.

[15] M. Hernandez and A. F. Frangi, "Non-parametric geodesic active regions: Method and evaluation for cerebral aneurysms segmentation in 3DRA and CTA," *Medical Image Analysis,* vol.11, pp. 224-241, 2007.

[16] N.D. Forkert, *et al.,* "Computer-aided nidus segmentation and angiographic characterization of arteriovenous malformations," in *International Journal of Computer Assisted Radiology and Surgery*, vol. 8, pp. 775-786, 2013.

[17] S. Bock, *et al,* "Robust vessel segmentation", *Proc. SPIE 6915, Medical Imaging 2008: Computer-Aided Diagnosis,* 2008.

[18] H. H. Chang *et al*., "Computer-assisted extraction of intracranial aneurysms on 3D rotational angiograms for computational fluid dynamics modeling", *Med.Phys.,* vol. 36(12), pp. 5612–5621, 2009.

[19] B. Preim and SB. Oeltze, "3D visualization of vasculature: an overview", *Visualization in medicine and life sciences,* pp. 39-59, 2008.

[20] I. Volkau *et al., "*On geometric modeling of the human intracranial venous system", *IEEE Trans Med Imag*, vol. 27(6), pp. 745-751, 2008.

[21] Y. Masutani *et al.,* "Region-growing-based feature extraction algorithm for tree-like objects", *Proc of visualization in biomedical computing,* pp. 161-171, 1996.

[22] C. Schumann *et al.,* "Model-free Surface Visualization of Vascular Trees", *EuroVis*, pp. 283-290. Eurographics Association, 2007.

[23] R. Gan, *et al.*, "Statistical cerebrovascular segmentation in three-dimensional rotational angiography based on maximum intensity projections," *Med. Phys.*, vol. 9, pp. 3017-3028, 2005.

[24] L. Vincent, "Morphological gray scale reconstruction in image analysis: Applications and efficient algorithms", *IEEE Transactions on Image Analysis*, vol. 2, pp. 176-201, 1993.

[25] Y. Huang, *et al.*, "A fast triangulation algorithm for 3D reconstruction from planar contours", *The International Journal of Advanced Manufacturing Technology*, vol. 24(1), pp. 98-101, 2004.